Subtle Design and Performance Comparison of WF-FSM and DC-VRM for Large-Scale Direct-Drive Wind Power Generation

Udochukwu B. Akuru
TSHWANE UNIVERSITY OF TECHNOLOGY
Department of Electrical Engineering
Pretoria, South Africa
E-Mail: AkuruUB@tut.ac.za

Maarten J. Kamper
STELLENBOSCH UNIVERSITY
Department of Electrical and Electronic Engineering
Cape Town, South Africa
E-Mail: kamper@sun.ac.za

Zi-Qiang Zhu
THE UNIVERSITY OF SHEFFIELD
Department of Electronic and Electrical Engineering
Sheffield, U.K.
E-Mail: z.q.zhu@sheffield.ac.uk

Acknowledgements

The work is supported in part by the Centre for Renewable and Sustainable Energy Studies (CRSES), Stellenbosch University, South Africa and Tshwane University of Technology, South Africa.

Keywords

«AC machine», «Brushless drive», «Design», «Finite-element analysis», «Wind-generator systems».

Abstract

We attempted the design and performance comparison of field-excited flux modulation machines viz., wound-field flux switching machine versus DC Vernier reluctance machine at large-scale power. Based on simple conceptual topologies and performance comparison using finite element analysis, preliminary findings at ~5.5 MW show potentials, while in-depth optimization is required for stiffer conclusions.

Introduction

Renewable energy is associated with notable credentials which include technological revolution, reduction in fossil fuel usage, climate change mitigation and economic empowerment, among others. Over the years, wind power has become a global reckoning force among new renewable energy electricity sources. Currently, the global cumulative total installed wind power generating capacity stands at 845 GW, with a 13.5 % growth experienced in the global wind power market in 2021 [1].

Considering the proliferation of wind power generation, wind generators are critical because they are integral drivetrain components in wind turbines [2]. In modern times, variable-speed wind turbines are preferred to fixed-speed because of extended operating power capture range [3]. The leading industrial wind generator technology is the variable-speed doubly fed induction generator (DFIG) using a three-stage high-speed gearbox (3G) drivetrain, meaning a smaller wind generator. However, DFIGs are besieged with low reliability due to its large-sized gearbox and brushed generators [3, 4, 5]. Due to large gearbox reliability constraints in high-speed wind generators, recent innovations have led to

single-stage (1G) or two-stage (2G) geared medium-speed wind generators. In effect, medium-speed wind generators yield a middle-point in terms of the size for both generator and gearbox. In some studies, the medium-speed drivetrain has been investigated for different wind generator concepts such as for DFIG, permanent magnet synchronous generator (PMSG) and wound-field flux switching machine (WF-FSM), providing the best tradeoff in terms of low cost of energy compared to other drivetrains [5-7].

In recent times, there is also the so-called direct-drive or gearless wind generator technologies which are gaining prominence because of total elimination of the gearbox. Direct-drive wind generators operate at very low speed and without gearboxes, meaning that the generators tend to increase dramatically in size and thus producing very high electromagnetic torque [3, 8]. To this end, direct-drive wind generators are prone to reduced generator torque density. Another issue with direct-drive generators is an enlarged airgap which is meant to reduce manufacturing challenges but at the same time, increases the cost and efficiency constraints of the generator because of the need for more excitation. To tackle some of these challenges, the mainstay wind generator technology for the direct-drive systems are PM machines which uses high-energy permanent magnets (PMs) for increased power density [9, 10]. But as identified in the recently published 5–year INNWIND.EU project which focused on design concepts for futuristic 10–20 MW offshore wind turbine drivetrains, PM drives based on a magnetic pseudo-direct drive (PDD) could be competitive in terms of lowering levelised cost of electricity (LCOE) but are notwithstanding vulnerable to the unpredictable market prices of PMs, among others [11].

Generally, it is believed that the future of wind turbines will be large-scale and offshore based [12]. This is because onshore systems have matured fully over the years with power rating and size limitations, exacerbated by huge logistics; whereas offshore wind turbines are not that limited [2]. This makes the variable-speed direct-driven PMSGs as the mainstay technology for this to happen. Notwithstanding, it is important to note that large offshore wind turbines operate remotely in harsher conditions compared to onshore systems; hence the cost of manufacturing, logistics and maintenance make them extremely difficult to manage. To this end, the important factors to consider in determining the appropriate wind generator technology for futuristic wind turbines should be electromagnetic output, mechanical design, thermal management, cost/size and reliability [3, 11].

Meanwhile, wound-rotor or electrically excited synchronous generator (WRSG) are being experimented for direct-drive wind generating systems. Such wind generator technologies have the advantage of having no PMs (i.e., no demagnetization threats and low-cost) as well as supplying adjustable reactive power and generator output voltage based on a variable field current excitation source but are known to be oversized and with reduced efficiency [2]. In addition, WRSGs often than not, require brushes and slip rings for their DC electromagnet exciters.

To this end, there are novel and emerging wound-field wind generator technologies which eliminate the need for brushes and slip rings to power their DC electromagnets, while offering a very robust rotor structure. They operate based on the principle of minimum reluctance or flux modulation effect to produce torque [13]. These machines typically comprise an armature, a field exciter and a flux modulator. Some examples of these brushless machines are the so-called stator-mounted flux modulation machines such as the DC field-excited double salient machines (DC-DSMs), DC field-excited flux reversal machines (DC-FRMs), wound-field flux switching machines (WF-FSMs) and DC-excited Vernier reluctance machines (DC-VRMs) [14-17], among others.

Currently, the so-called wound-field flux-modulation synchronous machines (e.g., WF-FSM and DC-VRM), has not received much consideration, unlike the conventional PMSG or WRSG [18, 19], for applications in MW wind power generation. WF-FSM for applications in wind generator drives have been demonstrated at industrial-scale power levels for geared medium-speed wind generators [17]. To the best of the authors, the DC-VRM have only been exhibited for small-scale direct-drive wind generators [20]. So far, it remains to be seen what the WF-FSM and DC-VRM would yield in terms of performance for MW-scale direct-drive wind generator systems. The study in this paper is a delicate

contemplation of such research adventure of which the WF-FSM and DC-VRM will be evaluated and compared for large-scale power direct-drive wind power generator systems. The study will be based on finite element analyses leading to small-scale experimental validation. For the proposed study, the overarching prioritization of these machine variants is due to their less emphasis on rare-earth materials for wind generator designs, as well as because of their robust design and high-power density compared to traditional wound-rotor machines [21, 22].

Topology Design Selection and Presentation

In this study, the three-phase 12/10 stator coils/rotor poles radial-flux concentrated winding machine topology is selected for both the WF-FSM and DC-VRM due to simplicity and optimum stator/rotor pole combinations [23, 24]. The generic machine models are presented in Fig. 1 as developed in 2D FEA software. As earlier indicated, both machines are benchmarked for direct (gearless) wind generator drivetrain at rotor speed of 12 r/min based on specifications laid out for a 5 MW direct-drive WRSG in [19].

The steady-state dq-axes generator modelling of both wound-field machine variants considered in this study, which fast-tracks the machine performance in FEA and where $I_d = 0$ control can be applied, has been undertaken previously in [25]; hence, it is not rehearsed here. Moreover, the in-house 2D FEA software utilised for this study applies position-stepping magnetostatic solutions which makes it highly efficient to undertake the proposed electromagnetic design analysis in MW-scale [26]. The research methodology for the study is summarized as shown in Fig. 2.

The technical specifications for the proposed machines are presented as shown in Table I. The specific dimensional parameters are sized approximate to sizing routines detailed in [27] and [20] for the WF-FSM and DC-VRM, respectively. Due to large-scale designs, approximations on end-windings are considered for the end-winding field and armature resistance. To facilitate a fair comparison of both generators, similar values have been imposed on the rated generator technical and dimensional characteristic data such as output power, stator outer diameter, airgap length and split ratio (ratio between stator airgap diameter to stator outer diameter), among others. To this end, the subtleness of the design process of the proposed MW-scale direct-drive wind generators is expressed in terms of the non-optimised designs, as well as inconsideration of the generator structural and thermal design aspects. The electromagnetic and design performance analysis now follows in the next section.

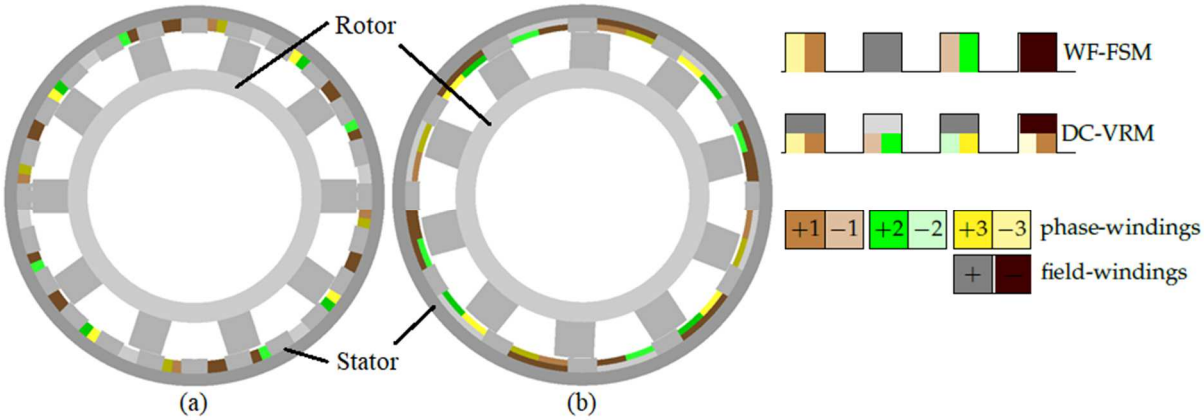

Fig. 1: Selected three-phase 12/10 stator coil/rotor poles machine topologies drawn in in-house FEM software: (a) WF-FSM, and (b) DC-VRM.

Fig. 2: Workflow of the research process.

Comparative Analysis of Electromagnetic and Design Performance

The no-load and on-load characteristics of the proposed machines are given first, thereafter the on-load characteristics. Figs. 3 and 4 presents the field lines and flux density vector diagrams of the designed machines under no-load conditions. As can be seen, high saturation, although much lower in the WF-FSM, is exhibited on the stator of both machines because of their stator-mounted configuration, besides the fact that optimization is yet to be undertaken. The airgap flux density waveforms of the designed machines under no-load conditions are shown in Fig. 5. The flux density in the WF-FSM design is much lower because of a higher split ratio which tends to minimize the DC loading in spite of a fixed current density compared to the DC-VRM.

In terms of the on-load performance, a summary is provided in Table II. The rated on-load average torque, as well as the generated power under rated conditions, are indicated; the latter approximates to 5.7 MW for both machines. The torque ripple values are seen to be slightly above 10%, which is very rough but considering that the machines are not optimized yet. The power factor of the DC-VRM is much lower compared to the WF-FSM, granted that the former naturally exhibits poor power fact due to its higher armature reaction effects in the Vernier machines' family [28]. For such direct drive designs, power factor is very critical because it Very interestingly, the evaluated efficiencies of these machines are quite high, especially for such wound-field machines. Although mechanical and other scant rotational losses have been ignored, the nearly lossless designs are quite remarkable considering that field winding losses are included. Based on the masses of the machines, which dwarfs 220 tons 7.5 MW, 10 r/min, direct-drive conventional wound-field generator as indicated in [19], it could have been expected that the core losses will dominate. But alas, the proposed machines end up with rated frequency of 2 Hz for evaluating the stator core losses, and even lower for the rotor [29]! Due to much lower pole number for the considered topology. Besides, the high efficiency is also indicative that the machines are oversized as indicated by their masses which may not be practical for the proposed wind turbine application, but with optimization, and selection of higher stator/rotor pole combination, the torque density of the machines can be potentially improved.

Table I: Design specifications of proposed direct-drive brushless wound-field wind generators

	WF-FSM	DC-VRM
Power	≥ 5 MW	
Line voltage	≈ 6 kV	
Speed	12 r/min	
Phase current density	1. 5A/mm^2	
Field current density	2.5 A/mm^2	
Stator outer diameter	8 m	
Airgap length	5 mm	
Shaft diameter	3 m	
Stack length	1.5 m	
Split ratio	0.8	
Slot fill factor	0.5	
Split ratio	0.85	0.8

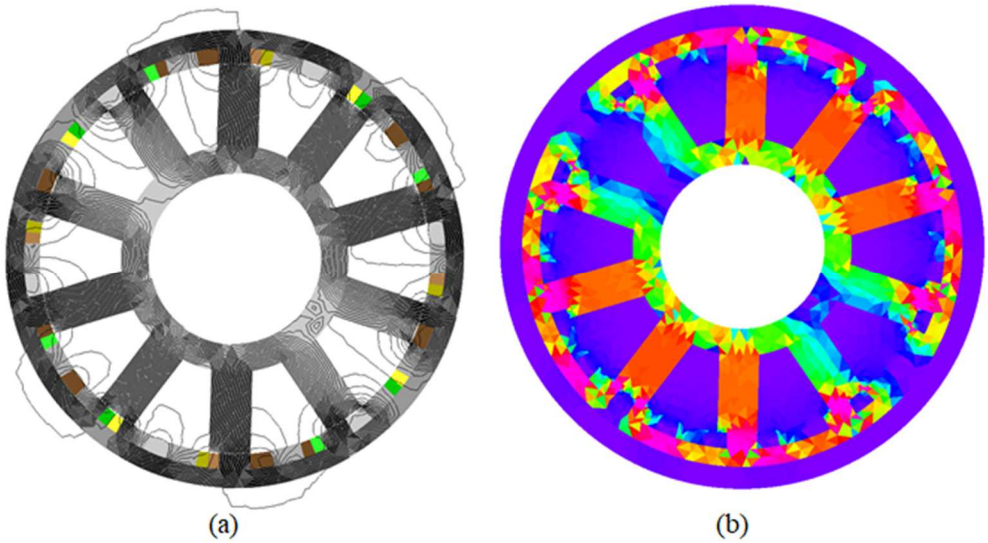

Fig. 3: WF-FSM: (a) flux lines, and (b) flux density map.

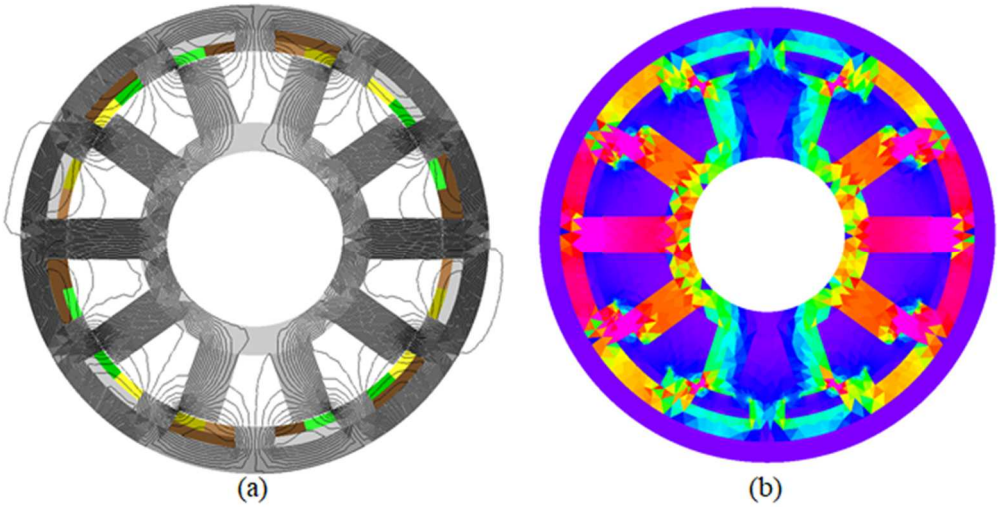

Fig. 4: DC-VRM: (a) flux lines, and (b) flux density map.

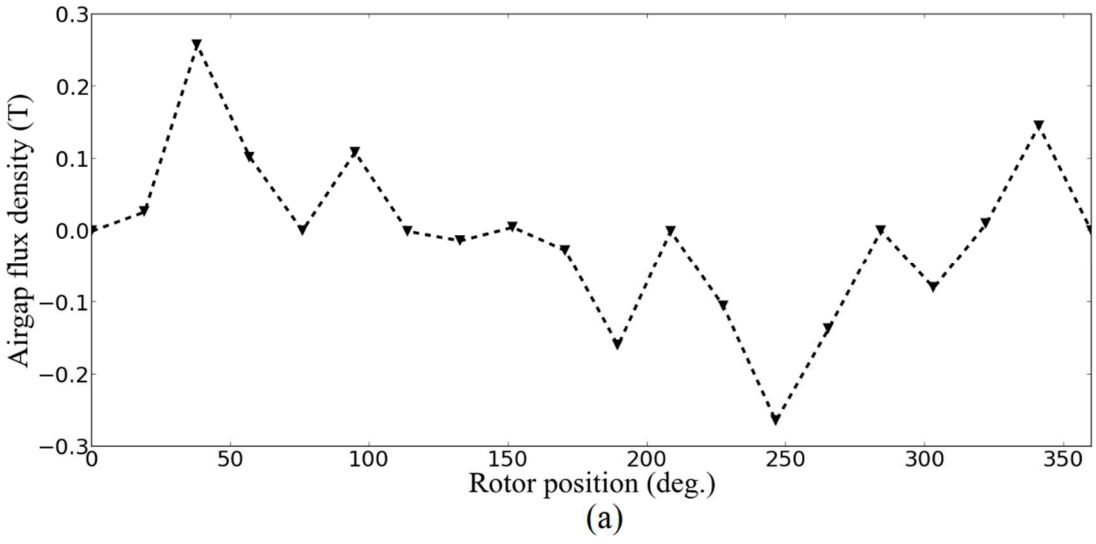

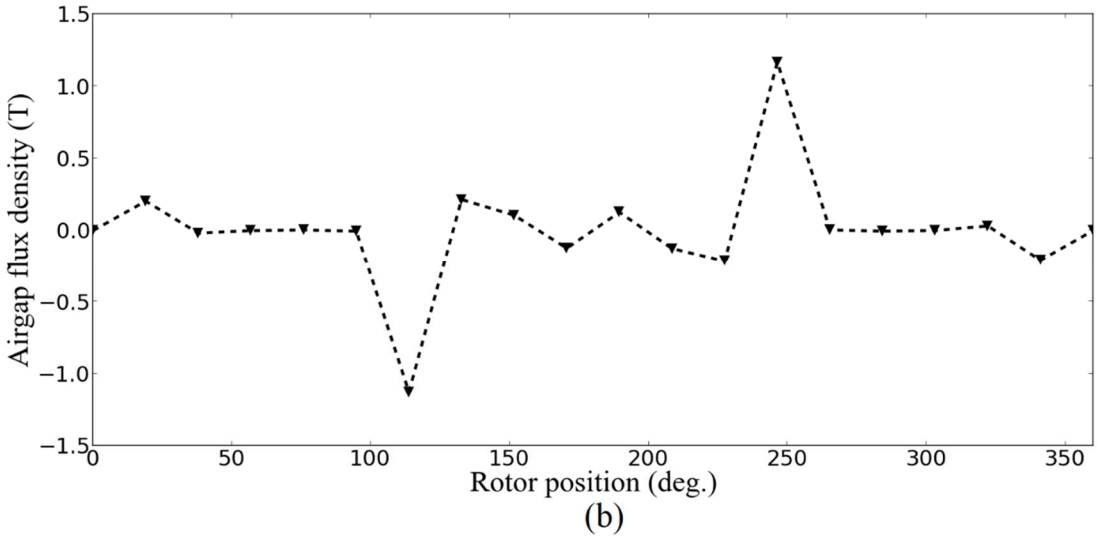

Fig. 5: No-load airgap flux density waveforms at rated field currents and 12 r/min: (a) WF-FSM (I_f = 0.97 kA), and (b) DC-VRM (I_f = 1.28 kA).

Table II: Comparative performance evaluation

	WF-FSM	DC-VRM
Power (MW)	5.8	5.7
Line voltage (kV)	6	6
Phase current (kA)	0.58	0.73
Field current (kA)	0.97	1.28
Torque (MNm)	4.6	4.5
Cogging torque (%)	11.32	12.6
Torque ripple (%)	10.7	12.5
Power factor	0.96	0.74
Core loss (kW)	11.0	9.2
Field Cu loss (kW)	5.60	4.04
Phase Cu loss (kW)	2.01	1.39
Efficiency (%)	99.7	99.7
Active mass (tons)	324	344
Torque/litre (kNm/m^3)	61.1	59.9
Loss density (kW/m^3)	0.24	0.22

Experimental Results

In this section, small experimental prototypes of the WF-FSM and DC-VRM are investigated at no-load to serve as modest proof of concepts. The machine design and rated parameters of both prototypes are presented in Table III. Both prototype machines are built for wind generator drives [17, 20]. Fig. 6 shows the experimental test benches for the prototype machines. The comparison of the no-load line voltages between FEA and measurement for both prototype machines is shown in Fig. 7. The disagreement between simulated and measured results is due to complications encountered during fabrication of the prototypes, especially for the WF-FSM, as well as fringing effects due to underestimation of so-called on-load induced DC winding induced voltages in predicted values [30].

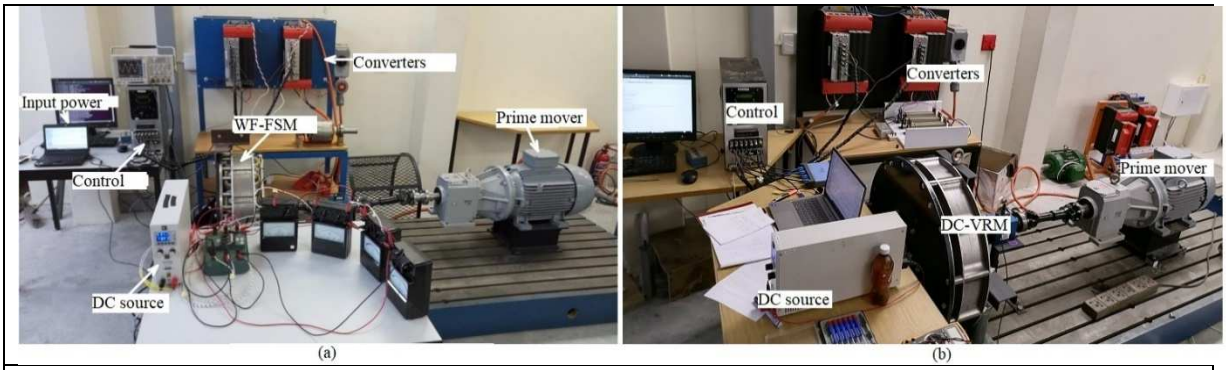

Fig. 6: Experimental set-up for prototype generators: (a) WF-FSM, and (b) DC-VRM.

Table III: Design and performance data for prototype generators

	WF-FSM	DC-VRM
Stator outer diameter (mm)	600	700
Rotor outer diameter (mm)	414.7	454.1
Stack length (mm)	104	109.6
Air gap thickness (mm)	0.7	0.8
Number of rotor poles	10	10
Number of stator slots	24	12
Rated speed (r/min)	360	200
Rated frequency (Hz)	60	33.3
Rated phase current (A)	9.8	27.5
Rated field current (A)	7.8	28.7
Rated line voltage (V)	700	384
Rated terminal power (kW)	10	14.6

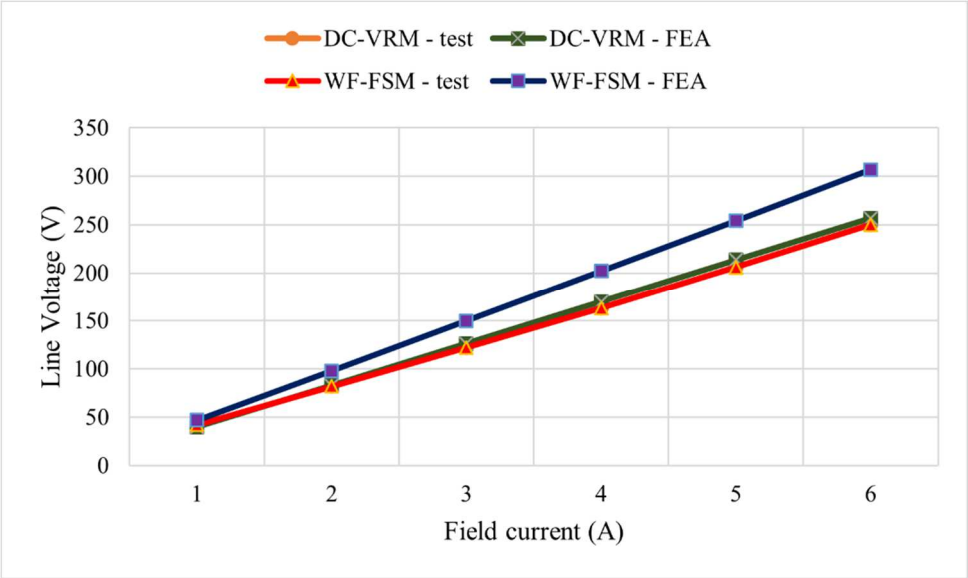

Fig. 7: Comparison of no-load voltages, WF-FSM@360 r/min and DC-VRM@300 r/min.

Conclusion and Future Work

In this study, conceptual WF-FSM and DC-VRM are designed, and their performance compared based on finite element analyses. Preliminary findings show the potentials of the design adventure, but the need for in-depth optimization is required for deeper conclusions to be made. At 5.5 MW, the resolved machines appear oversized for a 12/10 pole, 12 r/min designs, but appearing almost lossless at 99.7% efficiency. It must be reiterated that both machines have not been optimized, hence, the evaluated cogging torque and torque ripple ranged from 10% to 13%. Also, the torque per litre at approximately 60 kNm/m^3 and the active mass in excess of 300 tons are beyond standard ranges, due to the oversimplification of the airgap length, current density and selected stator/rotor pole design.

However, the design feasibility of the proposed machines for wind generator drives are validated based on existing small-scale prototypes. In future, additional studies would be undertaken to consolidate the design candidature of the highlighted MW-range stator-mounted brushless machines for direct-drive wind power systems through the following:

- Parametric variation on pole numbers, airgap length and current density on the overall generator performance.
- Multi-objective optimisation studies prioritising optimum torque density and torque performance.

References

[1] REN21, Renewables 2020 global status report Paris, 2020.
[2] Keysan O.: Future electrical generator technologies for offshore wind turbines, Wind Power, E&T IET Services, Aug 16, 2017.
[3] Chen H, Zuo Y, Chau K. T., Zhao W. and Lee C. H. T.: Modern electric machines and drives for wind power generation: A review of opportunities and challenges. IET RPG Journal, 15: pp. 1864-1887, 2021.
[4] Polinder H. Ferreira J. A., Jensen B. B., Abrahamsen A. B., Atallah K. and McMahon R. A. Trends in wind turbine generator systems, IEEE JESTPE Journal, Vol. 1 no 3, pp. 174–185, Sept. 2013.
[5] Zhu Z. Q. and Hu J.: Electrical machines and power-electronic systems for high-power wind energy generation applications: Part I—market penetration, current technology and advanced machine systems, COMPEL Journal, Vol. 32 no 1, pp.7–33, 2012.
[6] de Vries E.: The evolution of wind turbine drive systems, WINDPOWER Monthly, 26 April 2012.
[7] Akuru U. B. and Kamper M. J.: Design and investigation of low-cost PM flux switching machine for geared medium-speed wind energy applications, EPC&S Journal, Vol. 46 no 9, pp. 1082-1090, 2018.
[8] Li H., Chen Z. and Polinder H.: Research report on numerical evaluation of various variable speed wind generator systems, Project UpWind, Technical Report, 2006.

[9] Blaabjerg F. and Ionel D. M.: Renewable Energy Devices and Systems – State-of-the-Art Technology, Research and Development, Challenges and Future Trends, EPC&S journal, Vol. 43 no 12, pp. 1319-1328, 2015.
[10] Khan F., Sulaiman E. and Ahmad Md Z.: Review of switched flux wound-field machines technology, IETE Technical Review, Vol. 34 no 4, pp. 343-352, 2017.
[11] Jensen P. H., Chaviaropoulos T. and Natarajan A.: LCOE reduction for the next generation offshore wind turbines, INNWIND.EU PROJECT, October 2017.
[12] Bensalah A., Benhamida M. A., Barakat G. and Amara Y.: Large wind turbine generators: State-of-the-art review, ICEM 2018, pp. 2205-2211.
[13] Li D., Qu R. and Li J.: Topologies and analysis of flux-modulation machines, ECCE 2015, pp. 2153-2160.
[14] Udosen, D., Kalengo, K., Akuru U. B., Popoola O. and Munda J. L.: Non-Conventional, Non-Permanent Magnet Wind Generator Candidates, Wind Journal, Vol. 2, 429-450, 2022.
[15] Liu W., Wang H., Wang Y., Ren L. and Xiao L.: New approach to suppress torque ripple and improve torque output for wound-excited doubly salient machine, IECON 2016, pp. 2857-2861, 2016.
[16] Liu X. and Zhu Z. Q.: Electromagnetic performance of novel variable flux reluctance machines with DC-Field coil in stator, IEEE TransMag Journal, Vol. 49 no 6, pp. 3020-3028, Jun. 2013.
[17] Akuru U. B. and Kamper M. J.: Intriguing behavioral characteristics of rare-earth-free flux switching wind generators at small- and large-scale power levels, IEEE TIA journal, Vol. 54 no 6, pp. 5772-5782, Nov.-Dec. 2018.
[18] Stuebig C., Seibel A., Schleicher K., Haberjan L., Kloepzig M. and Ponick B.: Electromagnetic design of a 10 MW permanent magnet synchronous generator for wind turbine application, IEMDC 2015, pp. 1202-1208.
[19] Boldea I., Tutelea L. and Blaabjerg F.: High power wind generator designs with less or no PMs: An overview, ICEMS 2014, pp. 1-14.
[20] Akuru U. B., Kamper M. J. and Mabhula M.: Optimisation and design performance of a small-scale dc vernier reluctance machine for direct-drive wind generator drives, ECCE 2020, pp. 2965–2970.
[21] Pavel C. C., Lacal-Arántegui R., Marmier A., Schüler D., Tzimas E., Buchert M., Jenseit W. and Blagoeva D.: Substitution strategies for reducing the use of rare earths in wind turbines, Resources Policy, Vol. 52, pp. 349-357, 2017.
[22] Lee C. H. T., Chau K. T., Liu C. and Chan C. C.: Overview of magnetless brushless machines, IET EPA Journal, Vol. 12 no 8, pp. 1117-1125, 2018.
[23] Cheng M., Hua W., Zhang J. and Zhao W.: Overview of stator–permanent magnet brushless machines, IEEE TIE Journal, Vol. 58 no 11, pp. 5087–5101, Nov. 2011.
[24] Liu, X. and Zhu Z. Q.: Stator/rotor pole combinations and winding configurations of variable flux reluctance machines, IEEE TIA Journal, Vol. 50 no 6, pp. 3675-3684, Nov./Dec. 2014.
[25] Mabhula M., Akuru U. B. and Kamper M. J.: Cross-coupling inductance parameter estimation for more accurate performance evaluation of wound-field flux modulation machines, Electronics Journal, Vol. 9 no 11, August 2020.
[26] SEMFEM. Available: www0.sun.ac.za/semfem/index.html
[27] Akuru U. B. and Kamper M. J.: Formulation and multi-objective design optimisation of wound-field flux switching machines for wind energy drives, IEEE TIE Journal, vol. 65 no 2, pp. 1828-1836, 2017.
[28] Spooner E. and Haydock L.: Vernier hybrid machines, IEE Proc. EPA Journal, Vol. 150 no 6, 655-662, Nov. 2003.
[29] Fukami T., Avoki H., Shima K., Momiyama M., and Kawamura M.: Assessment of core losses in a flux-modulating synchronous machine, IEEE TIA Journal, Vol. 48 no 2, pp. 603-611, Mar./Apr. 2012.
[30] Wu Z., Zhu Z-Q., Wang C., Mipo J-C., Personnaz S. and Farah P.: Analysis and Reduction of On-Load DC Winding Induced Voltage in Wound Field Switched Flux Machines, IEEE TIE Journal, Vol. 67 no 4, pp. 2655-2666, April 2020.